Arab J Sci Eng (2014) 39:2107–2116
DOI 10.1007/s13369-013-0750-7

RESEARCH ARTICLE - MECHANICAL ENGINEERING

Experimental Investigation of the Vortex Generator Effects on a Gas Liquid Finned Tube Heat Exchanger Using Irreversibility Analysis

M. Ghazikhani · I. Khazaee · S. M. S. Monazzam · J. Taghipour

Received: 16 December 2011 / Accepted: 12 July 2013 / Published online: 5 September 2013

Abstract In the present work, the effect of wedge-shaped tetrahedral vortex generator (VG) on a gas liquid finned tube heat exchanger is experimentally investigated using irreversibility analysis. In this experiment, a wind tunnel system is used for forcing ambient air with mass flow rates of 0.047–0.072 kg/s across the finned tube heat exchanger. Hot water with constant flow rate of 240 L/h is circulated inside heat exchanger tubes at steady-state condition with inlet temperature range of 45–73 °C. The tests are carried out on the flat finned heat exchanger and then repeated on the VG finned heat exchanger. The results show that using mounted VGs lowered the air side irreversibility to heat transfer ratio (ASIHR) of heat exchanger. It is mainly because; the air side irreversibility decreases with heat transfer enhancement associated with lower temperature differences between air and water sides. To reveal the effects of these VGs on the heat exchanger, the VG performance based on air side irreversibility is quantified by the improved air side irreversibility to heat transfer ratio (IASIHR). The results indicate that the IASIHR is more than 1.05.

Keywords Finned tube heat exchanger · Irreversibility analysis · Vortex generator · Exergy effectiveness

M. Ghazikhani · S. M. S. Monazzam · J. Taghipour
Mechanical Engineering Department, Engineering Faculty, Ferdowsi University of Mashhad, P.O. Box 9177948944-1111, Mashhad, Iran

I. Khazaee (✉)
Department of Mechanical and Energy Engineering, Power and Water University of Technology, 16765-1719 Tehran, Iran
e-mail: imankhazaee@yahoo.com

I. Khazaee
Department of Mechanical Engineering, Torbat-e-jam branch, Islamic Azad University, Torbat-e-jam, Iran

الخلاصة

تم --في العمل الحالي التحقيق تجريبيا في تأثير مولد دوامة وتد ذي شكل رباعي السطوح (VG) في أنبوب مبادل زعانف حراري للغاز السائل باستخدام تحليل اللارجعة. وقد استُخدم في هذه التجربة نظام نفق الرياح لإجبار الهواء المحيط مع معدلات تدفق جماعي من0.047 إلى 0.072 كجم / ثانية المرور عبر زعانف أنبوب المبادل الحراري. وتم تدوير ماء ساخن مع معدل تدفق ثابت من 240 لتراً / ساعة داخل أنابيب المبادلات الحرارية في حالة الحالة المستقرة مع درجات حرارة مدخل من 45 إلى 73 درجة مئوية. وأجريت الاختبارات على مبادل حراري زعانف مستوٍ، ثم كررت التجربة على مبادل حراري زعانفVG . وأظهرت النتائج أن استخدام VGS المحملة خفضت لا رجعة الهواء الجانبية إلى نسبة نقل الحرارة (ASIHR) من المبادل الحراري، وهذا هو الأساس بسبب أن لا رجعة الهواء الجانبية تتناقص مع تعزيز نقل الحرارة المرتبط بانخفاض الاختلافات في درجة الحرارة بين جانبي الهواء والماء. وللكشف عن آثار VGS هذه على المبادل الحراري تم كميا قياس أداء VG على أساس لا رجعة الهواء الجانبية المحسنة إلى نسبة نقل الحرارة (IASIHR). وتشير النتائج إلى أن قيمة IASIHR هي أكثر من 1.05.

List of Symbols

ASIHR	Irreversibility to heat transfer ratio of air side
c	Specific heat of water (J/kg K)
c_{p}	Specific heat of air at constant pressure (J/kg K)
$\dot{E}$	Exergy transfer rate (W)
h	Enthalpy (J/kg)
$(h_2 - h_3)$	Air side pressure drop (mm w.g.)
IASIHR	Improved irreversibility to heat transfer ratio of air side
$\dot{I}$	Irreversibility rate (W)
$\dot{m}$	Mass flow rate (kg/s)
$\dot{Q}$	Heat transfer rate (W)
R	Gas constant (J/kg K)
s	Entropy (J/kg K)
T	Temperature (K)
VG	Vortex generator

Greek Symbols

$\Delta\dot{E}$	Change of exergy transfer rate (W)
ΔP	Pressure drop (Pa)
ΔT	Temperature difference (K)
$\Delta\varphi$	Change of specific flow exergy (J/kg)
$\varepsilon_{\text{exergy}}$	Exergy transfer effectiveness (%)
ε_{HE}	Heat exchanger effectiveness (%)
ν	Specific volume of water (m^3/kg)
φ	Specific flow exergy (J/kg)

Subscripts

a	Air
AS	Air side
HE	Heat exchanger
i	Inlet
max	Maximum possible
o	Outlet
w	Water
with VG	Heat exchanger with mounted VGs on its fin surfaces
without VG	Flat finned tube heat exchanger
0	The surrounding state

1 Introduction

Finned tube heat exchangers are extensively used in different fields such as power generation, refrigeration, air conditioning and automobile. For finned tube heat exchangers, the prevailing thermal resistance is at the air side [1]. Thus, for improving the performance of these heat exchangers, further heat transfer improvement of the fin surface is necessary. In order to decrease the thermal resistance on the air side, many variants of the fin models like wavy, slit, serrated, discrete ribs and louvered fins are commonly used. Junqi et al. [2] investigated a total of 11 cross-flow heat exchangers having wavy fin and flat tube experimentally. In their work the effects of fin pitch, fin height and fin length on the thermal hydraulic performance are examined. They found that the *j* and *f* factors decrease with increasing *Re*, in the tested range of *Re*, $Re = 800$–6,500. And the *j* and *f* factors increases with fin space increasing at the same *Re*.

Tao et al. [3,4] performed three-dimensional numerical simulations for laminar flow of wavy fin-and-tube heat exchangers by using body-fitted coordinates (BFC) method with fin efficiency effect accounted. They found that the local Nusselt number decreases along the air flow direction, but fin efficiency increases in general. They also found that the effects of the four factors on the heat transfer performance of the wavy fin-and-tube exchangers can be well described by the field synergy principle. Li et al. [5] investigated 3-D numerical simulation on laminar heat transfer and flow characteristics of a slit fin and tube heat exchanger with longitudinal vortex generators. They found that the Colburn *j*-factor and friction factor *f* of the novel heat exchanger with the novel slit fin is in between them under the same Reynolds number, and the factor *j*/(*f*1/3) of the novel heat exchanger increased by 15.8 and 4.2 %, respectively.

Peng and Ling [6] investigated the steady-state three-dimensional numerical models for predicting the thermal hydraulic performance for transverse direction (TD) and longitudinal direction (LD) flow through the serrated fins. They found that the local *Nu* values are greatest near the channel inlet and decrease rapidly through the flow directions shows the entrance effect in the LD and TD flow region.

Song et al. [7] investigated the flow and heat transfer in a finned flat tube heat exchanger with crossed discrete double incline dribs (CDDIR) numerically. They found that both the Nusselt numbers and friction factors increase with the rib height and decrease with the increase in grib pitch and the Nusselt number for the attack angle of $\alpha = 45$ is larger than for $\alpha = 30$ and $\alpha = 60$.

Nuntaphan et al. [8] investigated the effect of inclination angle on the louver finned tube heat exchanger subject to natural convection condition. They found that the inclination angle plays an importance role on the performance of the louver finned heat exchanger and the performance of the heat exchanger is associated with the interactions between fin, louver, tube, and inclination angle.

Dong et al. [9] investigated the air side heat transfer and pressure drop characteristics for 20 types of multi-louvered fin and flat tube heat exchangers. They found that at the same frontal velocity, heat transfer coefficients decrease with fin length and fin pitch increasing and fin height decreasing. The pressure drop decreases with fin length decreasing and fin pitch and fin height increasing at the same frontal velocity.

T'Joen et al. [10] investigated the flow within an interrupted fin design, the inclined louvered fin, experimentally through visualization. They found that the fin geometry had a very large impact on the transitional flow behavior, especially on vortex shedding.

One recently used approach for heat transfer improvement of the air side is to apply different VG patterns on the fin surfaces for inducing longitudinal vortices in the main flow. There are three mechanisms for heat transfer improvement of enhanced surfaces: developing boundary layers, swirling and flow destabilization. Applying VG has the important advantage of low cost and ease of achievement, with a typically modest pressure drop penalty [11–15].

In earlier studies, Chen et al. [11,12] investigated the effects of in-line and staggered punched longitudinal VGs on a finned oval tube. They found that staggered arrangement brought larger heat transfer enhancement than in-line arrangement since the longitudinal vortices influenced a larger area and intensified the fluid motion normal to the flow direction. Tian et al. [13] numerically investigated the effect of punched VGs on a wavy fin and tube heat exchanger with tubes in staggered and in-line arrangements. Their results showed that for in-line array the vortices developed downstream of VGs for a longer distance than the staggered array. There are some concerns about punched VG, for example the punched VG will cut the conduction paths in the fin. Zhang et al. [14] compared the heat transfer performance of finned tube bank with mounted and punched VGs. Their results declared that both of them had almost the same heat transfer and pressure drop results. Lei et al. [15] numerically investigated the effects of VGs on a novel heat exchanger. Their results indicated that the enhanced configuration produced the longitudinal vortices and accelerated the flow, which resulted in significant augmentations of heat transfer with modest pressure drop penalties.

In a recent study in 2010 Zeng et al. [16] numerically compared the influence of many parameters on the fin performance of a finned tube heat exchanger with delta winglet type VGs. They also optimized the effective parameters by Taguchi method. Their results confirmed that the factors related to the turbulence of air flow are very important parameters in the design of heat exchangers with the VG fin. They showed that the fin material and fin thickness have insignificant effect on the fin performance. Sanders and Thole [17] presented an experimental study on augmenting the heat transfer along the tube wall of the compact heat exchanger through the use of delta winglet type VGs placed on the louvers. In their attempt to optimize the winglet parameters, tube wall heat transfer augmentation as high as 39 % were achieved with associated friction factor augmentations as high as 23 %.

Wang et al. [18] presented the flow visualization of enlarged finned tube heat exchangers having in-line tube arrangements with and without the presence of wave type VGs. They showed that introducing the VGs brought about much better mixing characteristic accompanied with the frictional penalty of about 25–55 % higher than that of the plain fin geometry. They found that the penalty of pressure drops of the proposed VGs relative to plain fin geometry was relatively insensitive to change of Reynolds number.

Leu et al. [19] studied the effect of inclined block shape VGs mounted behind the tubes on the plate finned tube heat exchangers by numerical and experimental analysis. Their results indicated that the VGs enhanced the heat transfer by generating longitudinal vortices and aiding the fluid into the wake regions.

Tang et al. [20] experimentally investigated air side heat transfer and friction characteristics of five types of fin configurations of finned tube heat exchangers. They found that crimped spiral fin provided higher heat transfer and pressure drop than the other four fins. And also they presented that the heat exchanger with mixed fin (front VG fin and rear slit fin) had better performance than that of fin with delta wing VGs.

In a recent work, Henze and Wolfersdorf [21] investigated the influence of approach flow conditions on the heat transfer behind wedge-shaped tetrahedral VGs on a rectangular plate in a wind tunnel. Their results showed that the heat transfer enhancement depends on how deep the VG penetrates into the boundary layer. They confirmed that for regions which were affected by vortices the effect of turbulence intensity was less pronounced. They also found that increasing Reynolds number led to increasing heat transfer coefficients, whereas the heat transfer enhancement related to the smooth channel flow was decreasing. They also identified a correlation of the flow field and the heat transfer distribution.

In the present work, the experimental investigation of wedge-shaped tetrahedral VGs effect on a gas liquid finned tube heat exchanger is performed by irreversibility analysis. The VGs are connected to the fin surfaces at the upstream of air flow. The thermal performance of the original heat exchanger is compared with the improved one after mounting the VGs on its fin surfaces. To reveal the effects of these VGs on the heat exchanger, the VG performance based on air side irreversibility is quantified by the IASIHR which is the ratio of ASIHR of original heat exchanger to that of with mounted VGs.

2 Experimental Setup

Figure 1 shows a schematic sketch of the test facility used in this work. It consists of a wind tunnel system forcing air stream at room temperature flowing past the finned tube heat exchanger by a variable speed suction fan. The air duct is rectangular with 0.0317 m^2 cross-sectional area. Two differential micro-manometers are used; one for the measurement of air mass flow rate through the calibrated diaphragm and the other for the measurement of air pressure drop crossing the heat exchanger tubes. Also it consists of a hot water circulating loop. The water is supplied from the water reservoir with a float valve to the centrifugal pump for circulating through the loop. Then, it is heated by resistor type electric heater in the hot water accumulator. A rotameter is used for water flow measurement with a precision of ± 5 L/h. There is a bypass valve on the pump which is used to adjust and control the desired water flow rate in the loop. A U type Mercury differential manometer measures the pressure drop of water flow through the heat exchanger. The inlet and outlet temperatures of the hot water and cold air were measured using four

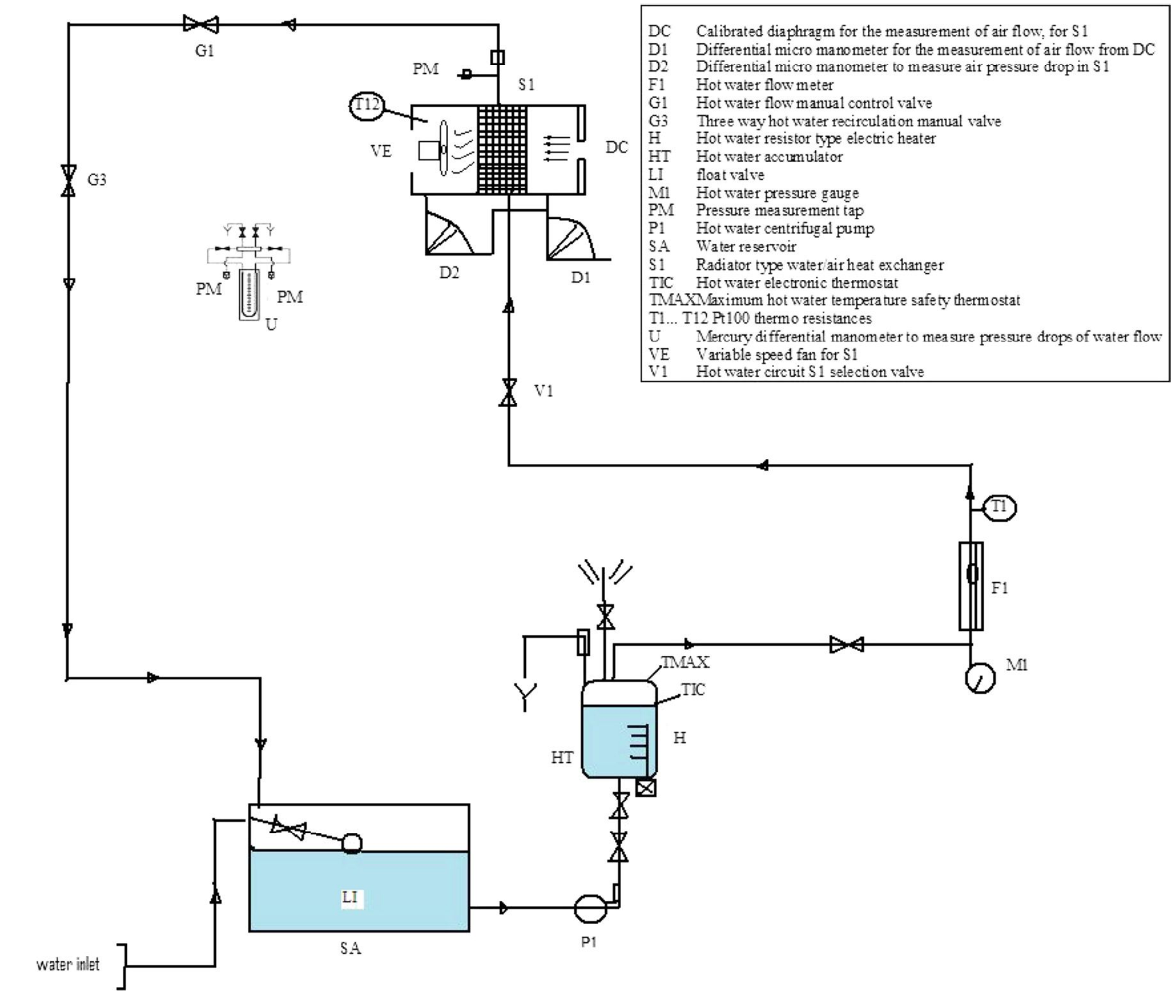

Fig. 1 Schematic sketch of the experimental setup (adopted from catalog of T60D-heat exchanger study unit of Didacta Italia co.)

Pt100 thermo-resistance thermocouples. The thermocouples are connected to a digital temperature recorder with a 0.1 °C resolution in the range 0.0–99.9 °C.

3 Test Section

The dimensions of the finned tube heat exchanger and the place of VGs on its fin surfaces is depicted in Fig. 2. It consists of 6 flat plate fins of 1 mm thickness and 16 copper pipes in two rows with in-line arrangement as the heat exchanger tubes. The tubes are of 1 mm thickness and outside diameter of 12.8 mm. It also consists of three collectors made of copper pipes of 28.7 mm outside diameter. It should be noted that the VGs are made of plastic and are mounted on the both sides of the fin surfaces.

Figure 3 shows the geometry and dimensions of one wedge-shaped tetrahedral VG used in this experiment. A schematic of the expected flow structure is also shown in this figure.

4 Testing Procedure

The ranges of the operating parameters are given in Table 1. At each experimental run, firstly, the water was heated to a desired temperature (in the range of 45–73 °C) in the heater and then the centrifugal pump was used to drive the hot water into the heat exchanger with fixed flow rate of 240 L/h. The ambient air flow was forced across the test section with air mass flow rates of 0.047, 0.060 and 0.072 kg/s. In general, it took about 1 h for the system to become stabilized, which was judged by the water inlet temperature fluctuation within 0.1 °C. After reaching the steady-state steady-flow conditions, the experimental data were recorded for subsequent test. In the present study, the water density was calculated at the water inlet temperature just after the rotameter. These experimental tests are carried out on the flat finned tube heat exchanger and then repeated on that of with mounted VGs.

All of the measurement apparatuses are operated under the identical condition for the original heat exchanger and

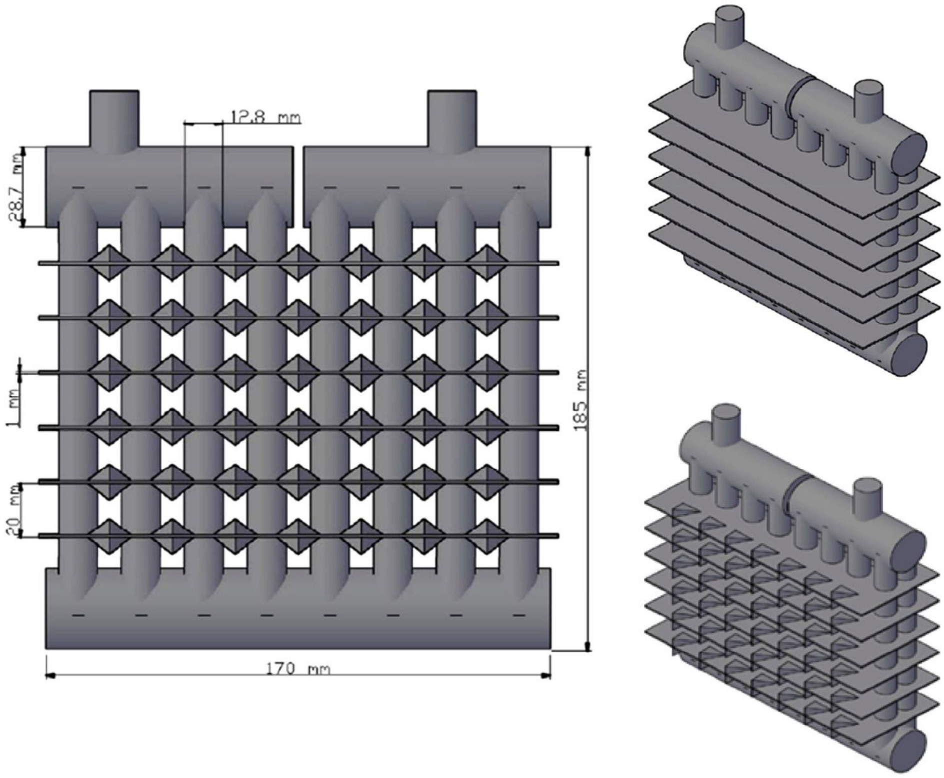

Fig. 2 The dimensions of the finned tube heat exchanger and the place of VGs on its fin surfaces

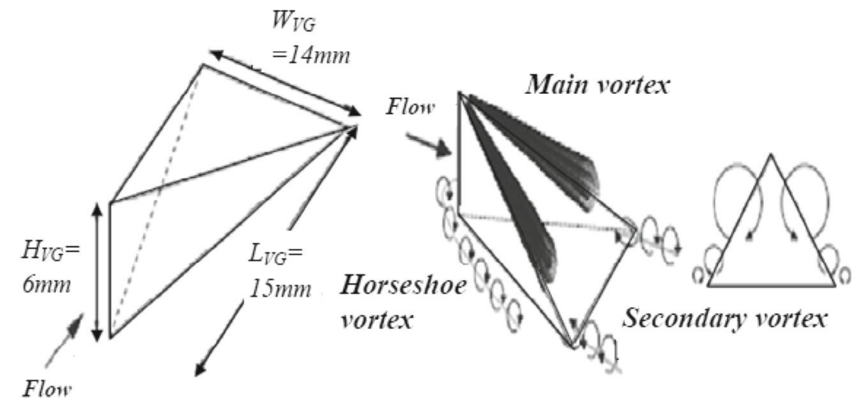

Fig. 3 Perspective and dimensions of tetrahedral wedge-shaped VG [21]

Table 1 Summary of tests performed

Experiment code	$\dot{m}_{\text{air}}$ (kg/s)	VGs used	Water flow rate (L/h)	T_{wi} (°C)	T_{ai} (°C)
WO1	0.047	No	240	45–73	14–15
WO2	0.060	No	240	45–73	14–15
WO3	0.072	No	240	45–73	13.5–15
WI1	0.047	Yes	240	45–73	15.5–17
WI2	0.060	Yes	240	45–73	15–16.5
WI3	0.072	Yes	240	45–73	16–17

the enhanced one; therefore, the experimental data are acceptable.

5 Data Analysis

The air mass flow rate in the duct is measured with a differential micro-manometer and orifice system. The mass flow rate of air is determined by using the chart of calibrated diaphragm. The air side pressure drop ΔP_{a} is also measured by another differential micro-manometer and is calculated by:

$$\Delta P_{\text{a}} = (h_2 - h_3) \times 9.80665 \tag{1}$$

where $(h_2 - h_3)$ is the micro-manometer reading.

The air side and the water side heat transfer rates of the heat exchanger can be evaluated by Eqs. (2a) and (2b), respectively:

$$\dot{Q}_{\mathrm{air}} = \dot{m}_{\mathrm{air}} c_{\mathrm{p}} (T_{\mathrm{ao}} - T_{\mathrm{ai}}) \tag{2a}$$
$$\dot{Q}_{\mathrm{water}} = \dot{m}_{\mathrm{water}} c (T_{\mathrm{wi}} - T_{\mathrm{wo}}) \tag{2b}$$

where $\dot{m}$ is mass flow rate; c is specific heat of water; and c_{p} is specific heat of air at constant pressure.

The heat transfer rate calculated by Eq. (2b) is not reliable, because the digital temperature meters have 0.1° resolution. This gives rise to 0.2° error of ΔT calculation. Although this calculation error brings about an undesirable error for water side heat transfer rate calculation, but it is acceptable for air side heat transfer rate calculation. This may be explained as in this experiment the temperature change of air stream is much greater than temperature change of water stream because the $\dot{m}_{\mathrm{air}} c_{\mathrm{p}}$ is much smaller than the $\dot{m}_{\mathrm{water}} c$. Therefore, the air side heat transfer rate calculation (by Eq. 2a) is used here rather than the water side.

The heat exchanger effectiveness $\varepsilon_{\mathrm{HE}}$ is defined as the ratio of actual heat transfer to the maximum heat transfer under idealized conditions which the outlet temperature of air is equal to the inlet temperature of water.

$$\varepsilon_{\mathrm{HE}} = \dot{Q}_{\mathrm{air}} / \dot{Q}_{\max} \tag{3}$$

where $\dot{Q}_{\max}$ is maximum possible heat transfer rate under limitations of the second law of thermodynamics and is calculated as follows:

$$\dot{Q}_{\max} = \dot{m}_{\mathrm{air}} c_{\mathrm{p}} (T_{\mathrm{wi}} - T_{\mathrm{ai}}) \tag{4}$$

Assuming that the heat transfer and flow processes are in steady state and heat leakage to the surroundings is negligible. In addition, the fluid physical properties are assumed to be constant. The specific flow exergy ϕ is calculated using the following equation:

$$\varphi = (h - h_0) - T_0 (s - s_0) \tag{5}$$

where h is enthalpy; s is entropy; and 0 indexes refer to the property at surrounding state. Then the change of exergy transfer rate of air and water derived by Wu et al. [22] can be calculated by Eqs. (6) and (7), respectively:

$$\Delta \dot{E}_{\mathrm{air}} = \dot{m}_{\mathrm{air}} \Delta \varphi_{\mathrm{air}} \tag{6}$$
$$\Delta \dot{E}_{\mathrm{water}} = \dot{m}_{\mathrm{water}} \Delta \varphi_{\mathrm{water}} \tag{7}$$

where

$$\begin{aligned} \Delta \varphi_{\mathrm{air}} &= c_{\mathrm{p}} (T_{\mathrm{ao}} - T_{\mathrm{ai}}) - T_0 (s_{\mathrm{ao}} - s_{\mathrm{ai}}) \\ &= c_{\mathrm{p}} (T_{\mathrm{ao}} - T_{\mathrm{ai}} - T_0 \ln(T_{\mathrm{ao}}/T_{\mathrm{ai}})) - T_0 R \Delta P_{\mathrm{a}} / P_{\mathrm{ai}} \end{aligned} \tag{8}$$

in which $\Delta P_{\mathrm{a}} / P_{\mathrm{ai}} \ll 1$, $\Delta P_{\mathrm{a}} = P_{\mathrm{ai}} - P_{\mathrm{ao}}$, and

$$\begin{aligned} \Delta \varphi_{\mathrm{water}} &= c (T_{\mathrm{wo}} - T_{\mathrm{wi}}) - T_0 (s_{\mathrm{wo}} - s_{\mathrm{wi}}) \\ &= c (T_{\mathrm{wo}} - T_{\mathrm{wi}} - T_0 \ln(T_{\mathrm{wo}}/T_{\mathrm{wi}})) - v \Delta P_w \end{aligned} \tag{9}$$

where R is gas constant; v is specific volume of water; and ΔP_{w} is pressure drop of water flow which is positive value.

It should be noted that in this calculations we consider the laboratory temperature equal to ambient temperature ($T_0 = 283$ K).

The exergy transfer effectiveness $\varepsilon_{\mathrm{exergy}}$ for this heat exchanger is determined by Eq. (10) [22].

$$\varepsilon_{\mathrm{exergy}} = \Delta \dot{E}_{\mathrm{air}} / \Delta \dot{E}_{\max,\mathrm{air}} \tag{10}$$

where

$$\Delta \dot{E}_{\max,\mathrm{air}} = \dot{m}_{\mathrm{air}} \left[c_{\mathrm{p}} (T_{\mathrm{wi}} - T_{\mathrm{ai}} - T_0 \ln(T_{\mathrm{wi}}/T_{\mathrm{ai}})) \right] \tag{11}$$

The irreversibility rate within the heat exchanger $\dot{I}_{\mathrm{HE}}$ is calculated by following equation:

$$\dot{I}_{\mathrm{HE}} = -\Delta \dot{E}_{\mathrm{water}} - \Delta \dot{E}_{\mathrm{air}} \tag{12}$$

The air side irreversibility rate $\dot{I}_{\mathrm{AS}}$ due to heat transfer and flow resistance can be calculated by Eq. 13:

$$\dot{I}_{\mathrm{AS}} = \dot{Q} (1 - T_0 / T_J) - \Delta \dot{E}_{\mathrm{air}} \tag{13}$$

where $T_J = (T_{\mathrm{wi}} + T_{\mathrm{wo}})/2$; and heat transfer rate $\dot{Q}$ is positive value.

The ASIHR is the amount of air side irreversibility rate for the unit of heat transfer rate in the heat exchanger.

$$\mathrm{ASIHR} = \dot{I}_{\mathrm{AS}} / \dot{Q} \tag{14}$$

The IASIHR is the ratio of the ASIHR of heat exchanger without VGs to that of the heat exchanger with VGs.

$$\mathrm{IASIHR} = \mathrm{ASIHR}_{\text{without VG}} / \mathrm{ASIHR}_{\text{with VG}} \tag{15}$$

6 Uncertainty Analysis

Uncertainty analysis is the part of risk assessment that focuses on the uncertainties in the assessment. Important components of uncertainty analysis include qualitative analysis that identifies the uncertainties, quantitative analysis of the effects of the uncertainties on the decision process, and communication of the uncertainty. The analysis of the uncertainty depends on the problem. Uncertainty in a measurement may be from the measurement module, measurement topics, liable of measurement and surround and they are investigated with statistical analysis. In this paper for uncertainty analysis of the experimental results, we repeat the experimental operation three times for each measuring parameters and use the average of them for analysis.

The uncertainty of the experimental results calculated from these equations:

$$\bar{x} = \frac{1}{n}\sum_{i=1}^{n} x_i \tag{16}$$

$$\sigma = \left[\frac{1}{n}\sum_{i=1}^{n}(x_i - \bar{x})^2\right]^{1/2} \tag{17}$$

$$\sigma_m = \frac{\sigma}{n^{0.5}} \tag{18}$$

that $\bar{x}$, σ and σ_m are average of experimental results, standard deviation and average of standard deviation. Therefore, for $n = 3$ the average of standard deviation is:

$$\sigma_m = 0.577\sigma \tag{19}$$

The percent of uncertainty of the experimental results is:

$$x = \frac{100\sigma_m}{\bar{x}} \tag{20}$$

For statistical analysis on the experimental results, we found that the average of percent of uncertainty for the T_{ao} and T_{wo} is 7.3 and 8.2 %.

7 Results and Discussion

In the present research, wedge-shaped tetrahedral VGs were used to generate longitudinal vortices over the fins of a gas liquid finned tube heat exchanger. Since for the finned tube heat exchangers, the prevailing thermal resistance is at the air side and the variation of the water flow rate has negligible effect on the thermal performance of the heat exchanger, in this experiment, the water flow rate is fixed.

Figure 3 shows a schematic of the expected flow structure around VG. It is perceived that on both backsliding edges of VG, two counter rotating longitudinal vortices are induced. These vortices make an enhanced heat transfer region behind the VG [21]. The flow around the rear edges of the VG leads to the secondary vortex, rotating in opposite direction than the adjacent main vortex. Finally, a smaller horseshoe vortex occurs by flow towards the front corners of VG attachment to the fin.

The variation of the heat transfer rate with water inlet temperature for different air mass flow rates is presented in Fig. 4 for the flat finned tube heat exchanger and VGs mounted on fin surfaces. It can be seen that the heat transfer rate increases with water inlet temperature due to higher temperature difference of air and water sides. Also, higher air mass flow rate results in greater heat transfer rate. This is due to the fact that larger air mass flow rates results in greater convective heat transfer coefficient of air side. In a word, air side Nusselt number is greater at higher air side Reynolds numbers. Furthermore, although the VGs are made of roughly insulated material, but using VGs increased the heat transfer rate for all the air mass flow rates. This may be explained

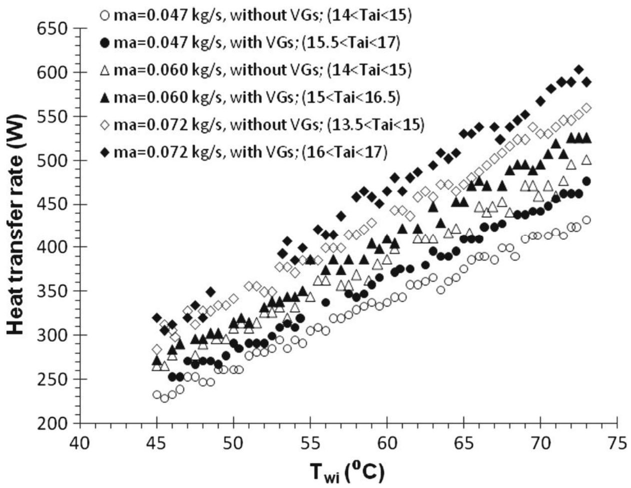

Fig. 4 The variation of heat transfer rate with water inlet temperature for flat finned heat exchanger and that of with mounted VGs at different air flows

as the heat transfer enhancement of fin and tube surfaces by longitudinal vortices generated by VGs connected to the fin surfaces at the upstream of air flow. The down sweep of these longitudinal vortices creates a secondary flow and disturbs the boundary layer growth, thereby results in heat transfer enhancement between the flowing fluid and fin surfaces. Furthermore, these vortices delay the boundary layer separation behind the tubes and remove the zones of poor heat transfer from the near wake of the tube which results in heat transfer enhancement of tube surfaces.

Figure 5 represents the rate of exergy destruction or irreversibility rate within the heat exchanger boundaries. From this figure, it is seen that the higher air mass flow rate results in greater irreversibility rates in comparison to the lower air mass flow rates; mainly because of increasing mean temperature differences between air and water sides. Also it is seen that the irreversibility rates are descended by using VGs, this is mainly due to heat transfer enhancement (as Fig. 4 shows) at lower temperature difference between air and water sides in the heat exchanger.

The prime cause of large temperature differences in this finned tube heat exchanger is the inertia of heat transfer to air side. Therefore normalizing the air side irreversibility rate with the heat transfer of the heat exchanger (i.e., ASIHR value) is an effective quantity to investigate the effect of VGs on the finned tube heat exchangers based on irreversibility analysis. Figure 6 represents the ASIHR variation for the flat finned heat exchanger and after using VGs on its fin surfaces. As is observed from this figure, the ASIHR increases with increasing water inlet temperature. This clarifies that although the heat transfer rate of heat exchanger increases with increasing water inlet temperature, its associated irreversibility rate increases much greater than its heat transfer augmentation. Also, it is perceived that the ASIHR value

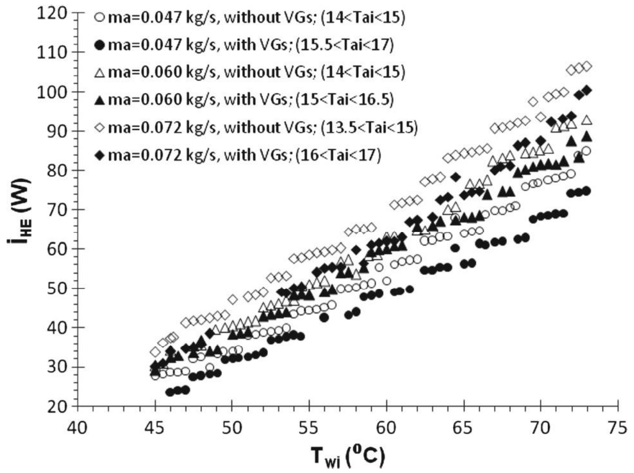

Fig. 5 The variation of irreversibility rate inside the heat exchanger with water inlet temperature for flat finned heat exchanger and that of with mounted VGs at different air flows

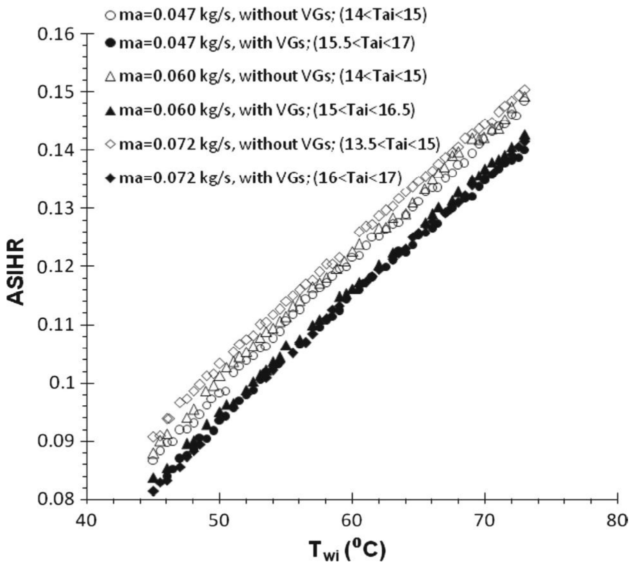

Fig. 6 The variation of ASIHR with water inlet temperature for flat finned heat exchanger and that of with mounted VGs at different air flows

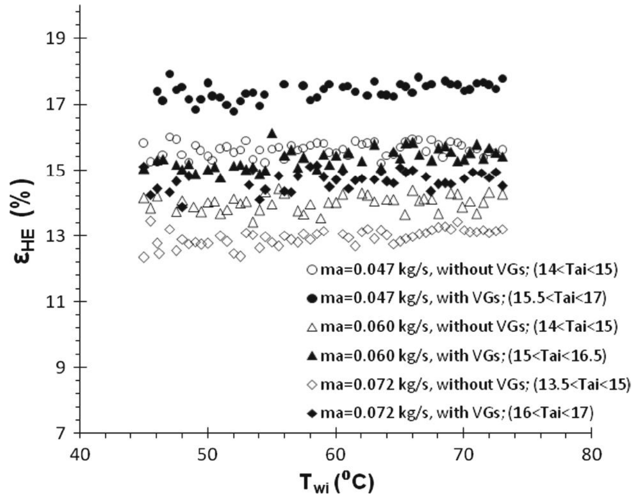

Fig. 7 The variation of heat exchanger effectiveness with water inlet temperature for flat finned heat exchanger and that of with mounted VGs at different air flows

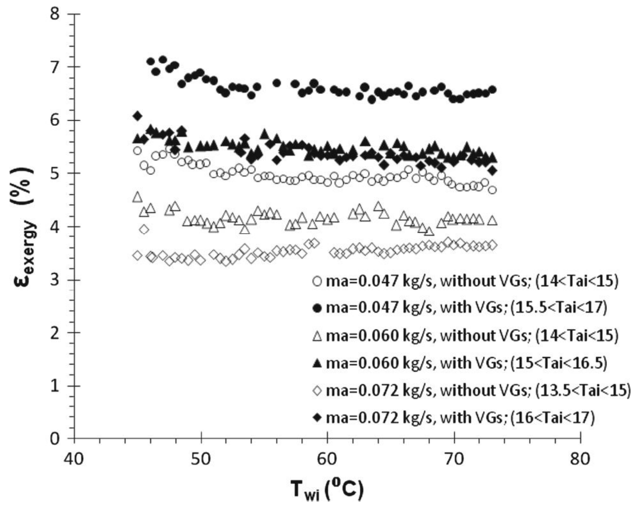

Fig. 8 The variation of exergy effectiveness of heat exchanger with water inlet temperature for flat finned heat exchanger and that of with mounted VGs at different air flows

is approximately irrespective of the air mass flow rate. Furthermore, using mounted VGs lowered the ASIHR of heat exchanger. It is mainly because the air side irreversibility decreases with heat transfer enhancement associated with lower temperature differences between air and water sides. Although, the VG makes special stream irreversibility due to inducing vortices in air flow, but the temperature difference of air and water sides is predominant factor for air side irreversibility.

Figure 7 shows the effectiveness of heat exchanger for the flat finned tube heat exchanger and after using VGs on its fin surfaces. It can be seen that the heat exchanger effectiveness ascended by using VGs due to increment of heat transfer rate to the air side of heat exchanger under the same inlet temperatures of air and water (i.e., by increasing of heat transfer rate under the same maximum possible heat transfer rate). Also, it is perceived that reduction of air mass flow rate leads to higher values of heat exchanger effectiveness. This may be explained as in smaller air mass flow rates, inlet air has more chance to close to the water inlet temperature. In other words, the temperature change of air stream and therefore outlet temperature of air will increase due to decreasing the heat capacity of air stream by decreasing air mass flow rate.

Figure 8 shows the exergy transfer effectiveness of heat exchanger. It can be seen that the values of exergy effectiveness have the similar trends with the heat exchanger effectiveness. The figure declared that the exergy transfer effectiveness ascended by using VGs. The main reason is that the

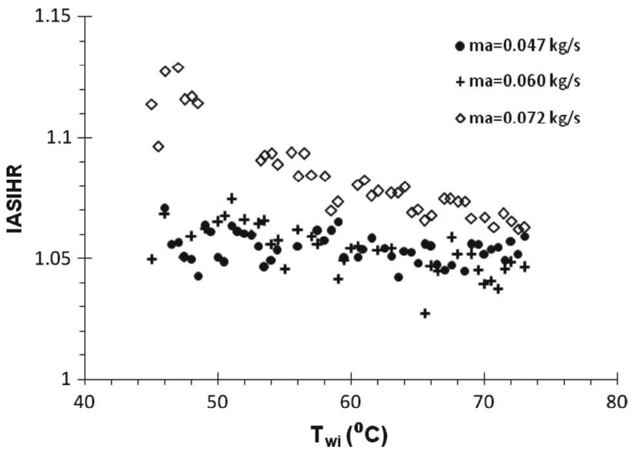

Fig. 9 The variation of IASIHR with water inlet temperature at different air flows

exergy transfer rate to the air side increases due to lower irreversibility rate within the heat exchanger at constant water inlet temperatures. In other words, under the same maximum possible exergy change of air, the exergy transfer rate to the air side increases. Also, it is perceived that reduction of air mass flow rate leads to higher values of exergy transfer effectiveness. This may be explained as in lower air mass flow rates, inlet air has more chance to close to the maximum possible exergy where the outlet temperature of air is equal to water inlet temperature.

To reveal the effects of these VGs on the heat exchanger, the VG performance based on air side irreversibility is quantified by the IASIHR which is the ratio of ASIHR of original heat exchanger to that of with mounted VGs. Figure 9 shows the IASIHR against water inlet temperature for different air mass flow rates. The results show that the IASIHR is greater than 1.05 for all air mass flow rates, which means that ASIHR for the initial heat exchanger is higher than 5 % greater than that of improved heat exchanger. This new parameter could be a useful interpretation of using VGs based on the second law of thermodynamics. In other words, the higher the amount of IASIHR more than unity shows better performance of VGs.

8 Conclusions

In this work, the experimental investigation of the effect of wedge-shaped tetrahedral VGs on a gas liquid finned tube heat exchanger was studied using irreversibility analysis.

The major conclusions are summarized as follows:

1. Using VGs induce counter-rotating longitudinal vortices on both backsliding edges. The down sweep of these longitudinal vortices creates a secondary flow and disturbs the boundary layer growth, thereby results in heat transfer enhancement between the flowing fluid and fin surfaces. Furthermore, these vortices delay the boundary layer separation behind the tubes and remove the zones of poor heat transfer from the near wake of the tube which results in heat transfer enhancement of tube surfaces. Therefore, although the VGs are made of insulated material, they are beneficial to the heat transfer enhancement of finned tube heat exchangers.
2. The exergy transfer effectiveness and the heat exchanger effectiveness have similar trends. Both of them increased on using VGs on the fin surfaces. Therefore, we conclude that this heat exchanger has much higher performances with VGs placed at the upstream of air flow.
3. Based on the irreversibility analysis, the amount of IASIHR shows how does VG work good? In other words, the amount of IASIHR shows the performance of a specified VG pattern used in the air side of a finned tube heat exchanger.
4. In this work, the IASIHR of tetrahedral VG is >1.05 for all operating conditions. This means that this enhancement technique reduced the air side irreversibility per unit heat transfer.

References

1. Kakaç, S.; Liu, H.: Heat Exchangers: Selection, Rating, and Thermal Design. CRC Press, New York (2002)
2. Junqi, D.; Jiangping, C.; Zhijiu, C.; Yimin, Z.; Wenfeng, Z.: Heat transfer and pressure drop correlations for the wavy fin and flat tube heat exchangers. Appl. Therm. Eng. **27**, 2066–2073 (2007)
3. Tao, Y.B.; He, Y.L.; Huang, J.; Wu, Z.G.; Tao, W.Q.: Numerical study of local heat transfer coefficient and fin efficiency of wavy fin-and-tube heat exchangers. Int. J. Therm. Sci. **46**, 768–778 (2007)
4. Tao, Y.B.; He, Y.L.; Huang, J.; Wu, Z.G.; Tao, W.Q.: Three-dimensional numerical study of wavy fin-and-tube heat exchangers and field synergy principle analysis. Int. J. Heat Mass Transf. **50**, 1163–1175 (2007)
5. Li, J.; Wang, S.; Chen, J.; Lei, Y.G.: Numerical study on a slit fin-and-tube heat exchanger with longitudinal vortex generators. Int. J. Heat Mass Transf. **54**, 1743–1751 (2011)
6. Peng, H.; Ling, X.: Analysis of heat transfer and flow characteristics over serrated fins with different flow directions. Energy Convers. Manag. **52**, 826–835 (2011)
7. Song, W.M.; Meng, J.A.; Li, Z.X.: Numerical study of air-side performance of a finned flat tube heat exchanger with crossed discrete double inclined ribs. Appl. Therm. Eng. **30**, 1797–1804 (2010)
8. Nuntaphan, A.; Vithayasai, S.; Kiatsiriroat, T.; Wang, C.C.: Effect of inclination angle on free convection thermal performance of louver finned heat exchanger. Int. J. Heat Mass Transf. **50**, 361–366 (2007)
9. Dong, J.; Chen, J.; Chen, Z.; Zhang, W.; Zhou, Y.: Heat transfer and pressure drop correlations for the multi-louvered fin compact heat exchangers. Energy Convers. Manag. **48**, 1506–1515 (2007)
10. T'Joen, C.; Jacobi, A.; De Paepe, M.: Flow visualization in inclined louvered fins. Exp. Therm. Fluid Sci. **33**, 664–674 (2009)
11. Chen, Y.; Fiebig, M.; Mitra, N.Y.: Heat transfer enhancement of a finned oval tube with punched longitudinal vortex generators in-line. Int. J. Heat Mass Transf. **41**, 4151–4166 (1998)

12. Chen, Y.; Fiebig, M.; Mitra, N.Y.: Heat transfer enhancement of finned oval tubes with staggered punched longitudinal vortex generators. Int. J. Heat Mass Transf. **43**, 417–435 (2000)
13. Tian, L.; He, Y.; Tao, Y.; Tao, W.: A comparative study on the air-side performance of wavy fin-and-tube heat exchanger with punched delta winglets in staggered and in-line arrangements. Int. J. Therm. Sci. **48**, 1765–1776 (2009)
14. Zhang, Y.H.; Wu, X.; Wang, L.B.; Song, K.W.; Dong, Y.X.; Liu, S.: Comparison of heat transfer performance of tube bank fin with mounted vortex generators to tube bank fin with punched vortex generators. Exp. Therm. Fluid Sci. **33**, 58–66 (2008)
15. Lei, Y.G.; He, Y.L.; Tian, L.T.; Chu, P.; Tao, W.Q.: Hydrodynamics and heat transfer characteristics of a novel heat exchanger with delta-winglet vortex generators. Chem. Eng. Sci. **65**, 1551–1562 (2010)
16. Zeng, M.; Tang, L.H.; Lin, M.; Wang, Q.W.: Optimization of heat exchangers with vortex-generator fin by Taguchi method. Appl. Therm. Eng. **30**, 1775–1783 (2010)
17. Sanders, P.A.; Thole, K.A.: Effects of winglets to augment tube wall heat transfer in louvered fin heat exchangers. Int. J. Heat Mass Transf. **49**, 4058–4069 (2006)
18. Wang, C.C.; Lo, J.; Lin, Y.T.; Liu, M.S.: Flow visualization of wave-type vortex generators having inline fin-tube arrangement. Int. J. Heat Mass Transf. **45**, 1933–1944 (2002)
19. Leu, J.S.; Wu, Y.H.; Yang, J.J.: Heat transfer and fluid flow analysis in plate-fin and tube heat exchangers with a pair of block shape vortex generators. Int. J. Heat Mass Transf. **47**, 4327– 4338 (2004)
20. Tang, L.H.; Zeng, M.; Wang, Q.W.: Experimental and numerical investigation on air-side performance of fin-and-tube heat exchangers with various fin patterns. Exp. Therm. Fluid Sci. **33**, 818–827 (2009)
21. Henze, M.; von Wolfersdorf, J.: Influence of approach flow conditions on heat transfer behind vortex generators. Int. J. Heat Mass Transf. **54**, 279–287 (2011)
22. Wu, S.Y.; Yuan, X.F.; Li, Y.R.; Xiao, L.: Exergy transfer effectiveness on heat exchanger for finite pressure drop. Energy **32**, 2110–2120 (2007)